Accepted Manuscript

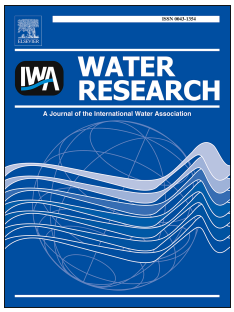

Ozone and chlorine reactions with dissolved organic matter - Assessment of oxidant-reactive moieties by optical measurements and the electron donating capacities

Linda Önnby, Elisabeth Salhi, Garrett McKay, Fernando L. Rosario-Ortiz, Urs von Gunten

PII: S0043-1354(18)30519-0

DOI: 10.1016/j.watres.2018.06.059

Reference: WR 13886

To appear in: *Water Research*

Received Date: 19 March 2018

Revised Date: 8 June 2018

Accepted Date: 24 June 2018

Please cite this article as: Önnby, L., Salhi, E., McKay, G., Rosario-Ortiz, F.L., von Gunten, U., Ozone and chlorine reactions with dissolved organic matter - Assessment of oxidant-reactive moieties by optical measurements and the electron donating capacities, *Water Research* (2018), doi: 10.1016/j.watres.2018.06.059.

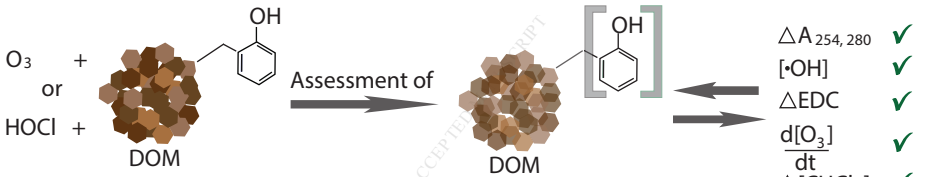
O3 +
or
HOCl +
OH
DOM
Assessment of
OH
DOM
△A 254, 280
[•OH]
△EDC
d[O3]
dt
△[CHCl3]

Ozone and chlorine reactions with dissolved organic matter - assessment of oxidant-reactive moieties by optical measurements and the electron donating capacities

Linda Önnby[a], Elisabeth Salhi[a], Garrett McKay[b], Fernando L. Rosario-Ortiz[b], Urs von Gunten[a, c, d*]

[a]Eawag, Swiss Federal Institute of Aquatic Science and Technology (EAWAG), 8600 Dübendorf, Switzerland

[b]Department of Civil, Environmental and Architectural Engineering, Environmental Engineering Program, University of Colorado, Boulder, USA

[c]Institute of Biogeochemistry and Pollutant Dynamics, Swiss Federal Institute of Technology (ETH) Zürich, 8092 Zürich, Switzerland

[d] School of Architecture, Civil & Environmental Engineering (ENAC), Ecole Polytechnique Fédérale de Lausanne (EPFL), 1015 Lausanne, Switzerland

Corresponding author: Urs von Gunten
Email: vongunten@eawag.ch
phone: +41 58 765 5270

Abstract

Oxidation processes are impacted by the type, concentration and reactivity of the dissolved organic matter (DOM). In this study, the reactions between various types of DOM (Suwannee River fulvic acid, Nordic Reservoir NOM and Pony Lake fulvic acid) and two oxidants (ozone and chlorine) were studied in the pH range 2-9 by using a combination of optical measurements and electron donating capacities.

The relationships between residual electron donating capacity (EDC) and residual absorbance showed a strong pH dependence for the ozone-DOM reactions with phenolic functional groups being the main reacting moieties. Relative EDC and absorbance abatements (UV_{254} or UV_{280}) were similar at pH 2. At pH 7 or 9, the relative abatement of EDC was more pronounced than for absorbance, which could be explained by the formation of UV-absorbing products such as benzoquinone from the transformation of phenolic moieties. An increase in fluorescence abatement with increasing pH was also observed during ozonation. The increase in fluorescence quantum yields could not be attributed to formation of benzoquinone, but related to a faster abatement of phenolic moieties relative to fluorophores with low ozone reactivity.

The overall $^{\bullet}OH$ yields as a result of DOM-induced ozone consumption increased significantly with increasing pH, which could be related to the higher reactivity of phenolic moieties at higher pH. The $^{\bullet}OH$ yields for SRFA and PLFA were proportional to the phenolic contents, whereas for NNOM, the $^{\bullet}OH$ yield was about 30% higher.

During chlorination of DOM at pH 7 an efficient relative EDC abatement was observed whereas the relative absorbance abatement was much less pronounced. This is

43 due to the formation of chlorophenolic moieties, which exert a significant absorbance,
44 and partly lose their electron donating capacity.

45 Pre-ozonation of SRFA leads to a decrease of chloroform and haloacetic acid
46 formation, however, only after an threshold of > ~50% abatement of the EDC and under
47 conditions which are not precursor limited. The decrease in chloroform and haloacetic
48 acid formation after the threshold EDC abtement was proportional to the relative
49 residual EDC.

50 **Keywords:** Dissolved organic matter, electron donating capacity, oxidant reactivity,
51 ozone, chlorine, disinfection by-products

52 **1. Introduction**

53 *1.1 Role and properties of DOM in natural and engineered aquatic systems*

54 Dissolved organic matter (DOM) plays an important role in numerous natural
55 and engineered aquatic processes. DOM consists of a mixture of heterogenous
56 compounds with a continuum of functional groups and molecular sizes (Leenheer and
57 Croue 2003). DOM contains organic molecular structure with a wide size range,
58 including humic substances, biopolymers, building blocks and low molecular weight
59 organic acids (Huber et al. 2011, Leenheer and Croue 2003).

60 In water treatment, DOM is typically characterized by measurements of
61 concentration (dissolved organic carbon, DOC) and/or optical properties (absorbance or
62 fluorescence). Absorbance has been used as a surrogate for DOM concentration and as a
63 process control parameter for the oxidation of organic contaminants in water and
64 wastewater treatment (Gerrity et al. 2012, Wittmer et al. 2015). DOM is often
65 characterized by the specific ultraviolet absorbance at 254 nm ($SUVA_{254}$, UV
66 absorbance divided by the DOC), a surrogate for DOM aromaticity (Weishaar et al.

2003). Over the last years, the use of DOM fluorescence measurements has become more common. These measurements were used to quantify both DOM concentration and character in natural and engineered systems (Gerrity et al. 2012, Osburn et al. 2012, Stedmon et al. 2003).

1.2. Role and change of the DOM in oxidative water treatment processes

During oxidative processes (e.g., application of ozone or chlorine), DOM is the main sink for the added oxidants. Specific functional groups within the DOM (e.g. poly(phenols), amines, olefins, anilines, etc.) are susceptible to chemical modifications during exposure of the DOM to oxidants (Lee and von Gunten 2010). The reactivities and concentrations of such moieties in the DOM determine the extent of the DOM-oxidant interactions and their effects on the targeted oxidation/disinfection processes (Lee and von Gunten 2010).

Some understanding of the interactions between the oxidants and DOM can be gained by considering reaction rate constants between a specific oxidant and known DOM moieties. For example, the apparent second order rate constant for the reaction between ozone and phenol is on the order of 10^6 $M^{-1}s^{-1}$ at pH 7, whereas for chlorine (HOCl) it is 20 $M^{-1}s^{-1}$ (Deborde and von Gunten 2008, Gallard and von Gunten 2002). Given that the aromaticity (i.e., average proportion of aromatic moieties including phenolic moieties to the total carbon) varies between 12-22 % for DOM isolates, a phenol concentration of approximately 2 x 10^{-6} M can be estimated for for a 1 mg C/L solution of SRFA. This suggests that an equimolar concentration of ozone will be consumed within seconds, whereas the HOCl consumption will take five hours.

Changes in selected physicochemical properties of DOM during its reaction between ozone or HOCl are well-characterized. For example, the overall absorbance

and fluorescence intensities decrease with increasing extent of chemical oxidation (Gerrity et al. 2012). Concomitantly, the reaction of the oxidants with DOM result in the formation of disinfection by-products (DBPs) (Lee et al. 2007, Mitch and Sedlak 2002, von Gunten 2003), and also changes in the redox properties of the DOM (Wenk et al. 2013). Depending on the oxidant applied, different types of DBPs can be formed. Primary products from the attack of phenolic by ozone are benzoquinones, catchechols, muconic acids, etc. (Mvula and von Sonntag 2003, Ramseier and von Gunten 2009, Tentscher 2018), which can be further oxidized to aldehydes, ketones and carboxylic acids (Hammes et al. 2006). For chlorination, primary products from phenolic moieties are chlorophenols, which are then further transformed to trihalomethanes (e.g., chloroform) or haloacetic acids (Gallard and von Gunten 2002, Ge et al. 2014). In addition, both ozone and chlorine can react with amines, forming e.g., nitroso- and nitro-compounds or *N*-oxides or organic and inorganic halamines, respectively (de Vera et al. 2017b, Heeb et al. 2017, McCurry et al. 2016, von Sonntag and von Gunten 2012).

1.3 Characterizing the redox properties of the DOM and assessing DBPs formation

Recently, there has been a growing interest in the electrochemical properties of DOM in water treatment applications. A method based on mediated electrochemical oxidation employing $ABTS^{\bullet+}$ - the one-electron oxidation product of ABTS (2,2'-azino-bis(3-ethylbenzothiazoline-6-sulphonicacid) – as an electron transfer mediator to facilitate electron transfer from oxidizable moieties in the DOM to the working electronde of the electrochemical cell (Aeschbacher et al. 2010). The outcome of this measurement is the so-called electron donating capacity (EDC). A further development of this method involved automation by implementing flow-injection analysis in which electron donation from the DOM to $ABTS^{\bullet+}$ under formation of ABTS was quantified chronoamperometrically in an electrochemical flow cell (Walpen et al. 2016). In

116 another study, EDC was measured employing size-exclusion chromatography for DOM
117 size separation, followed by the same approach involving $ABTS^{\bullet+}$ for EDC
118 quantification by a post-column reaction and spectrophotometric analysis of the
119 decolourization of $ABTS^{\bullet+}$ to ABTS (Chon et al. 2015, Önnby et al. 2018).

120 EDC measurements allow for an assessment of the redox properties or the
121 antioxidant capacity of the DOM (Aeschbacher et al. 2010). Known electron-donating
122 moieties of the DOM include phenols such as mono- and poly-hydroxylated benzene
123 rings, amines, aniline, sulfur or olefinic moieties. Previous work has shown that the
124 EDC values of ten DOM isolates were positively correlated with their titrated phenol
125 contents, strongly suggesting that phenolic moieties of the DOM are major contributors
126 to the EDC of DOM samples (Aeschbacher et al. 2012).

127 Taken together, the extent of the oxidant consumption and the formation of
128 DBPs from the oxidant-DOM reactions depend on the concentrations and types of the
129 reactive moieties in DOM. Combined EDC and absorbance measurements have
130 advanced the understanding of the DOM-ozone and the DOM-chlorine reactions (Wenk
131 et al. 2013), including the effects on micropollutant abatement (Chon et al. 2015, de
132 Vera et al. 2017a).

133 The main objective of this paper is to advance our understanding of the reactions
134 between oxidants (ozone and chlorine) and DOM. To investigate changes in the DOM
135 during oxidation, changes in EDC and optical properties (absorbance and fluorescence)
136 were assessed at various pH values for dosage and kinetic experiments. Furthermore,
137 the formation of hydroxyl radicals ($^{\bullet}OH$) was investigated during ozonation of DOM.
138 Finally, the formation of chloroform and chloroacetic acids without or with pre-
139 ozonation followed by chlorination was measured and related to the abatement of the

EDC.

2. Material and methods

2.1. Chemicals, natural organic matter isolates, preparation of solutions

A list of the chemicals and standards used in this study is provided in Text S1, in the supplementary data.

Model DOM isolates including Suwanee River fulvic acid (SRFA), Nordic Reservoir NOM (NNOM) and Pony Lake fulvic acid (PLFA) were obtained from the International Humic Substances Society (IHSS) (details are given in Table S1). The type and composition of all solutions used in this study, including preparation details, are provided in Text S2 and Table S2.

2.2 Oxidation experiments

Ozonation was performed as dosage experiments (50 mL) or kinetic experiments (5 to 250 mL), in absence or in presence of 100 mM *t*-BuOH as a hydroxyl radical (•OH) scavenger (Staehelin and Hoigné 1985). Control experiments showed that the added *t*-BuOH did not interfere with absorbance measurements at 254 nm nor with the quantification of the EDC (Table S3).

For ozone dosage experiments, samples that had been ozonated were stored at room temperature overnight to ensure complete ozone depletion. For kinetic experiments, 5 mL samples were collected using a dispenser system (Hoigné and Bader 1994) and immediately quenched by various quenchers (see below) at pre-determined reaction times up to 3000s. Samples corresponding to 5, 10 and 15s were obtained from separate experiments performed in 15 mL glass vials with a 5 mL reaction volume and direct quenching (see below).

Chlorine dosage experiments were performed with 40 mL samples. After chlorine addition, the samples were stored for 48h at room temperature for complete depletion of chlorine. The samples were stored in the dark to avoid photo-decomposition of chlorine (Nowell and Hoigné 1992).

In dosage experiments, specific ozone doses of 0 - 0.5 mmol O_3/mmol C or specific chlorine doses of 0 - 0.2 mmol HOCl/mmol C were applied. The specific oxidant doses lie within the typical range applied in water and wastewater treatment of (Bourgin et al. 2018, Garcia-Villanova et al. 1997, Zimmermann et al. 2011). For some selected experiments, SRFA was pre-ozonated with higher specific ozone doses than above (0 - 2.0 mmol O_3/mmol C) to obtain an EDC abatement of ≤ 95%. Thereafter, the samples were treated with the above specific chlorine doses, to follow the conventional treatment step undertaken at water treatment plants with pre-ozonation and post-chlorination.

Kinetic ozone experiments were performed with a specific ozone dose of 0.25 mmol O_3/mmol C. Depending on the subsequent measurements (see sections 2.4.1 - 2.4.4), ozone in the kinetic experiments was quenched by either (i) indigo to quantify residual ozone, (ii) maleic acid to quantify the EDC, or (iii) sulfite to quench ozone to quantify $^{\cdot}$OH formation and to measure solution absorbance spectra (control measurements are shown in Table S3).

2.2.1 Quantification of the formation of $^{\bullet}$OH during ozone depletion

$^{\bullet}$OH is formed by various pathways during ozone decomposition in water (von Sonntag and von Gunten 2012). The use of *t*-BuOH as $^{\bullet}$OH quencher results in the formation of formaldehyde (Flyunt et al. 2003). Two moles of formaldehyde are formed from the reaction of one mole of $^{\cdot}$OH with *t*-BuOH (Flyunt et al. 2003).

187 *2.2.2 Optical measurements*

188 Absorbance spectra (200 to 600 nm) were measured on Uvikon 940 (Kontron
189 Instruments) or Varian Cary 100 (Agilent Technologies) instruments in quartz cuvettes
190 (1 and 5 cm path lengths). The spectra were collected at least two hours after addition of
191 the oxidant (kinetic experiments) or after resting overnight (ozone) or 48h (chlorine), to
192 ensure that the oxidants were completely consumed. Fluorescence absorbance was
193 collected in duplicate with a Fluoromax-4 spectrofluorometer (Horiba, USA) for
194 ozonated or non-ozonated samples. Fluorescence emission was collected between 300-
195 700 nm at excitation wavelengths between 240-550 nm using a 0.25s integration time
196 and a 5 nm bandpass. Spectra were corrected for inner filter effects and normalized to
197 Raman area (at Ex=350 nm) in Matlab. Fluorescence quantum yields were calculated
198 using quinine sulfate (in 0.05 M H_2SO_4) as a reference based on a previously reported
199 method (Cawley et al. 2014). To confirm that measurements from ozone-dosed samples
200 prepared in the two involved laboratories resulted in identical conditions, the respective
201 absorbance spectra were compared. This comparison indicated good agreement between
202 the experimental protocols of the two laboratories (Figure S1) allowing for comparison
203 of EDC and fluorescence spectra collected in the first and second laboratory,
204 respectively.

205 *2.2.3 Quantification of the EDC by SEC-EDC*

206 EDC was quantified following the method described in detail elsewhere (Chon
207 et al. 2015, Önnby et al. 2018). In brief, the method consists of size exclusion
208 chromatography (SEC) followed by a post-column reaction (PCR) of DOM with the
209 radical cation of ABTS ($ABTS^{\bullet+}$) as a chemical oxidant, which was pre-formed by
210 oxidation of ABTS with chlorine (Pinkernell 2000). The SEC-EDC system leads to a

molecular size fractionation of DOM prior to its oxidation of electron-donating moieties in the DOM by $ABTS^{\bullet+}$. The resulting reductive decolorization of $ABTS^{\bullet+}$ (absorbance maximum at 405 nm) to ABTS (no absorbance at 405 nm) is then quantified by monitoring absorbance at this wavelength using a spectrophotometric flow-through detector. A more detailed description of the method is given in Text S3 and in (Önnby et al. 2018).

2.2.4 Analytical methods

The concentration of formaldehyde was determined colorimetrically using the Hantzsch reaction (Nash 1953). The quantified samples were in the concentration range of 5-200 µM, with a quantification limit of 0.5 µM formaldehyde. The obtained molar absorption coefficient at 412 nm of formaldehyde was 7207 $M^{-1}cm^{-1}$. Reported concentrations were average values from triplicate measurements with a residual standard deviation (RSD) < 5%. The exact concentration of a commercial formaldehyde solution used as a calibration standard for the colometric method was determined by volumetric titration with sulfuric acid in a solution containing formaldehyde and sodium sulfite (Walker 1944).

Ozone depletion was followed by measuring the residual ozone concentration using the indigo method (Bader and Hoigné 1981). Briefly, a 2 mM indigo solution and a 0.02 M phosphate buffer reagent was added and diluted prior to use by ensuring that indigo was present in a stoichiometric excess (at least twofold) to ozone and measured at 600 nm in quartz cuvettes (1 and 5 cm path lengths).

Chloroform formed during reaction of DOM with HOCl was quantified by gas chromatography-mass spectrometry (GC-MS, GC-8000 Fisions) with head-space injection (Combi-PAL). Samples (5 mL) were filled in 10 mL head space vials, which

were pre-equilibrated at 80°C for 30 min prior to injection, following a previous protocol (Shah et al. 2015). Haloacetic acids (HAAs) were measured using a capillary ion chromatography (Thermo Dionex ICS-4000) coupled to tandem mass spectrometry (Thermo TSQ-Vantage) with an injection volume of 100 µL (Shah et al. 2015). More details about the two anlytical methods for chloroform and HAAs quantification, including method detection limits, measuring ranges and RSD values (%) are given in Text S4.

3. Results and discussion

3.1. Estimation of phenol concentrations

The aromaticity for the chosen DOM isolates was obtained from the IHSS (cf. Table S1) and a certain fraction of the aromatic units are phenolic moieties. In this study, we quantified the EDC abatement for DOM isolates treated with specific ozone doses between 0.05 and 0.15 mmol O_3/mmol C. A linear response in EDC abatement (EDC/EDC_0) as a function of the specific ozone dose was observed (Figure S2). The calculated EDC abatement was then correlated with the previous relationship between EDC and phenol (Aeschbacher et al. 2012) according to Text S5.

Table 1 summarizes the phenol content determined from EDC measurements, the aromaticity obtained from the IHSS, respectively, and the nitrogen content for SRFA, NNOM and PLFA. The quantified phenol contents based on EDC measurements show a similar trend as the aromaticity from the IHSS. The quantified phenolic content for SRFA and PLFA were well correlated with the values for phenolic content given by IHSS (IHSS 2017). It is observed that the phenol content decreased in the order SRFA > NNOM > PLFA. Table 1 shows that the absolute EDC of PLFA is lower (2.43 mmol e^- /g C) compared to the EDC of SRFA or NNOM, respectively (5.98 and 4.16 mmol e^-/g

259 C) (Aeschbacher et al. 2012).

260 (Table 1)

261 *3.2 pH dependence of the ozone consumption kinetics upon reaction with the three model*
262 *DOM isolates*

263 Figure 1 shows the kinetics of the ozone depletion in solutions containing either
264 SRFA, NNOM or PLFA as a function of pH in presence of *t*-BuOH to quench $^{\bullet}OH$.
265 Generally, the rates of the ozone depletion decreased with decreasing pH, which is a
266 consequence of the lower reactivity of protonated organic moiteies with ozone (von
267 Sonntag and von Gunten 2012). At pH 2, ozone was still detectable after 3000s (roughly
268 ~10% for SRFA, ~20% for NNOM and PLFA (overlapping data points) of the initially
269 added ozone). For pH 3, less than 5% of the initially added ozone was detectable after
270 3000s of reaction with SRFA and NNOM, whereas the ozone residual was still about
271 20% of the initially added ozone for PLFA. At pH 7 or 9, ozone depletion was
272 significantly faster. At pH 9, ozone was completely consumed within 60s of its addition
273 to SRFA and NNOM solutions, respectively, and only 10% residual ozone was detected
274 for PLFA. The pronounced decrease in ozone reactivity with increasing pH can be
275 rationalized by DOM moieties that undergo acid-base speciation (e.g., phenols and/or
276 amines). These are typically less or non-reactive in their neutral/protonated forms,
277 which is the case at pH 2 (Lee and von Gunten 2010). For example, apparent second
278 order rate constants for the reaction between ozone and phenol increases from 10^3 to 10^8
279 $M^{-1}s^{-1}$ when the pH is increased from pH 2 to 9 (Lee and von Gunten 2010). For
280 amines, the apparent second order rate constants are very low for the protonated species,
281 whereas they are much higher (between 10^4 and 10^6 $M^{-1}s^{-1}$) for neutral amines (Lee and
282 von Gunten 2016, von Sonntag and von Gunten 2012).

Based on the higher phenolic/aromatic and the lower nitrogen proportion of SRFA and NNOM compared to PLFA (Table 1), we hypothesize that the observed increase in ozone depletion rate with increasing pH was due to the reaction with deprotonated phenolic moieties. In contrast, PLFA has lower phenol contents and more nitrogen-containing moieties such as amines, which are present in higher proportions (6.51 %N, Table 1) and might play a certain role for the pH-dependence of the slower observed ozone depletion kinetics in the PLFA experiments. To this end, it was demonstrated in a recent study that the nitrate formation from amine moieties in PLFA increased relative to the absorbance abatement (phenolic moieties) with increasing pH (Song et al. 2017). This finding indicated that there was a higher contribution of nitrogen-containing moiteies to the ozone consumption in PLFA as compared to SRFA. Regardless of similar concentrations between phenol and amine moieties, phenolic moieties will always outcompete amines in the DOM-ozone interactions. However, due to the high amine reactivity at higher pH, it will be difficult to resolve the two individual effects kinetically in batch-type experiments with ozone.

(Figure 1)

3.3 Kinetics of EDC/EDC$_0$ abatement during oxidation

Figure S3 shows the kinetics of the relative EDC (EDC/EDC$_0$) abatement during ozonation of SRFA, NNOM and PLFA in the pH range 2 - 9. The decrease in EDC/EDC$_0$ during ozonation increased with increasing pH. These results suggest that EDC-active sites react more efficiently at a higher pH, which is in accordance with the faster ozone depletion discussed in section 3.2. Based on the correlation of EDC with DOM phenolic content, this result provides additional evidence for the importance of phenolic moieties in DOM in the consumption of ozone by DOM.

3.4. Kinetics of absorbance abatement during oxidation

Changes in absorbance spectra during ozonation of SRFA, NNOM and PLFA are shown in Figures S4 – S7 for experiments at pH 2, 3, 7 and 9, respectively. The largest absorbance changes were observed over the wavelength range 220-280 nm. Although experiments at all pHs showed a fast initial abatement in DOM absorbance, the abatement was strongly pH dependent. At pH 2 and 3, the absorbance decreases occured over the entire reaction time of 3000s (Figures S4 and S5). At pH 7, the absorbance abatement is significant for the initial 100s, followed by a slower and gradual decrease until 1000s (Figure S6). For pH 9, the absorbance abatement occurred very rapidly after ozone addition, with no further decrease in absorbance at longer reaction times (Figure S7).

3.5 Relationships between changes in EDC and absorbance

Previous studies investigated the relationships between the relative abatements of EDC and absorbance during DOM chemical oxidation only at circumneutral pH (Chon et al. 2015, Önnby et al. 2018, Wenk et al. 2013). Figures 2a-d show the relative abatement in both EDC and absorbances during ozonation of SRFA in the pH range 2-9. Figures S8 and S9 show the analogous relationships for the same pH range for NNOM and PLFA (absorbance at 254 nm) and for SRFA, NNOM and PLFA (absorbance at 280 nm), respectively. At low pH, ozonation resulted in comparable relative decreases of EDC and absorbance (i.e., data close to the 1:1 line in Figures 2a-b). By comparison, at high pH the relative EDC abatement increases compared to the relative absorbance abatement (data to the left of the 1:1 line in Figures 2c-d).

330 The decerase in EDC/EDC_0 compared to the relative absorbance abatement with
331 increasing pH may have resulted from a higher extent of benzoquinone formation from
332 phenolic moieties at higher than lower pH (Mvula and von Sonntag 2003, Ramseier and
333 von Gunten 2009, Tentscher and von Gunten 2017, Tentscher et al. 2018). These
334 benzoquinone moieties in the DOM also absorb light at 254 nm and would therefore
335 have led to a smaller decrease in the absorbance at 254 nm at high pH. The formation of
336 benzoquinones would thus be consistent with the observed shifts in the correlations
337 (EDC/EDC0 vs A/A_o) towards smaller decerases in absorbance values in these plots.
338 At lower pH, the yield of benzoquinones from the phenol-ozone reaction is smaller with
339 a higher yield of ring-opening products such as acetic, formic and maleic acids with low
340 UV absorbance (Ramseier and von Gunten 2009). Hence, ozonation of DOM at the low
341 pH resulted in limited formation of UV-absorbing moieties and thus a comparable
342 relative decrease of the absorbance (total aromatics) and EDC (phenols, a subset of the
343 aromatic moieties). Consistent with this explanation, the data collected for SRFA,
344 NNOM and PLFA at low pH fell close to the 1:1 lines in Figures 2, S8 and S9.

345 **(Figure 2)**
346

To further elucidate the reasons for the observed correlations between the relative abatements of EDC and absorbance, changes in absorbance spectra were investigated with phenol as a surrogate for phenolic moieties in the DOM. For these experiments, we did not quantify EDC for phenol as this low-molecular weight compound will not be detectable in the SEC-EDC set-up due to its small molecular size. Figures 3a-c show the changes in absorbance spectra for the reactions between ozone (52 µM) and phenol (34 µM) yielding a similar molar ozone:carbon ratio as in Figure 2 (0.25:1.0). Absorbance spectra for reaction times of 0 and 60s are shown (completion of the reaction) in Figure 3 for pH 2, 3 and 7. Figures 3b and 3c also include the spectra of 1,4-benzoquinone at pH 3 and pH 7 for comparison. The added 1,4-benzoquinone concentrations in Figures 3b and 3c are 10 µM for pH 3 and 21 µM for pH 7, respectively.

Figures 3a-c show that, as the pH increased, oxidation of phenol via ozone led to an enhanced formation of an absorbance peak centered at a maximum of about 252 nm. The good agreement with lambda max at 252 nm suggest that 1,4-benzoquinone was formed in these experiments, both at pH 3 and pH 7. This conclusion is supported by an earlier study which used HPLC analyses to demosntrate that the ozonation of phenols results in 1,4-benzoquinone formation (Ramseier and von Gunten 2009, Tentscher et al. 2018). Based on the above-mentioned concentrations of formed benzoquinone, the calculated yields relative to the initial phenol concentration were 17% at pH 3 and 40% at pH 7, which is comparable to previous findings (Mvula and von Sonntag 2003, Ramseier and von Gunten 2009, Tentscher et al. 2018).

In parallel with the development of an absorbance peak at 252 nm, the absorbance at 272 nm increased at pH 7, while it decreased at pH 3 during ozonation of phenol (compare Figures 3b-c). These results suggest that phenolic polimerization products are possibly formed during ozonation of phenol at pH 7 giving rise to the absorbance increase at 272 nm.

Overall, the absorbance at 254 nm increases during ozonation of phenol at all pH values and under the experimental conditions used herein. However, the increase was smaller at lower pH values. Because phenols are only a subset of chromophores in DOM, the results obtained from phenol ozonation can only be applied to the ozonation of DOM in a qualitative manner. Despite this limitation, the overall trend of the DOM experiments above, where an increased absorbance peak was formed at 254 nm at high pH due to formation of 1,4-benzoquinone from phenolic moieties in DOM, can partially be explained by the smaller formation of UV-absorbing moieties at lower pH. Overall, a deviation from the 1:1 correlation (Figures 2c-d) is partially caused by the formation of benzoquinone-type compounds, which still absorb light but are more electron defficient and hence, lead to an enhanced relative EDC abatement compared to the absorbance.

(Figure 3)

3.6 Changes of fluorescence of DOM during DOM ozonation

3.6.1 Changes in fluorescence intensity as a function of ozone dose and experimental pH

In addition to evaluating the absorbance, the changes in fluorescence were also considered. Fluorescence offers an additional tool to assess the contribution of different moieties of the DOM towards the observed reactivity with ozone. The fluorescence intensity of DOM has previously been shown to decrease with increased ozone dose

393 (Gerrity et al. 2012). As an example, oxidation of phenols and formation of
394 benzoquinone should result in a decrease in fluorescence intensity due to the very weak
395 fluorescence of benzoquinones (Ma et al. 2010). The decrease is explained by
396 destruction of chromophoric (aromatic) moieties (Swietlik and Sikorska 2004). Figure
397 S10 shows that both the relative fluorescence intensity and the relative absorbances for
398 SRFA and PLFA decreased with an increasing specific ozone dose at pH 3, 7 and 9,
399 respectively. Overall, the decrease in fluorescence was less pronounced compared to the
400 loss in absorbance, indicating that light-absorbing moieties were more sensitive to
401 ozone oxidation than fluorescent moieties (see below).

402 *3.6.2 Changes in fluorescence quantum yields of DOM with increasing*
403 *ozonation*

404 The de-coupling of the absorbance and fluorescence responses to oxidation by
405 ozone was further studied by measuring the fluorescence quantum yields (Φ_f). The Φ_f
406 describes the probability of the excited singlet state within DOM to be deactivated
407 through flourescence, relative to non-radiative pathways (Lakowicz 2006). Φ_f was
408 calculated as the integrated emission spectrum divided by the absorbance at a particular
409 excitation wavelength (Cawley et al. 2014). The Φ_f were investigated for ozonated
410 SRFA and PLFA in the pH range 3 - 9. Figure S11, shows how Φ_f generally increase
411 continuously with specific ozone doses for SRFA and PLFA at all pH values. The
412 extent of the observed Φ_f increase depends on both the type of DOM as well as the pH.
413 In contrast to PLFA, an induction period was apparent for SRFA at pH 7 and 9 (but not
414 at pH 3). The values for Φ_f did not significantly change compared to non-ozonated
415 DOM up to a specific ozone dose of 0.05 mmol O_3/mmol C.

416 Figures 4a and 4b show the relative changes in absorbance and Φ_f (at λ_{Ex} = 350

nm, relative to samples without ozonation) for PLFA and SRFA as a function of the specific ozone dose or the residual EDC, respectively. For PLFA, absorbance and Φ_f respond immediately to changes in specific ozone doses (Figure 4a). For SRFA, the Φ_f increases more steadily as a function of the specific ozone dose or the relative EDC abatement (Figures 4a and b).

(Figure 4)

The increase in Φ_f with increasing ozone exposure seemingly contradicts the prediction based on current models of DOM photophysics (Sharpless and Blough 2014). Benzoquinones are known not to fluoresce, and it could be expected that a conversion of phenolic moieties to benzoquinones as a result of ozone-DOM reactions as discussed above, would lead to lower Φ_f. Additionally, considering the charge transfer (CT) model for fluorescence, the overall quantum yield would decrease due to the loss of electron donors (i.e., phenols), thereby reducing the abundance of CT bands. However, a recent study suggests that CT intereactions are not the main photophysical mechanism within DOM, and therefore the observed results should be considered in the context of individual compounds (McKay et al. 2018).

The effect of ozone on both absorbance and fluorescence (i.e., decrease in intensity while observeing an increase in Φ_f) can be explained as follows. Ozone treatment of the DOM resulted in the loss of both light absorbing and fluorescent moieties, including phenols. In the case of absorption, the abatement of these moieties still leaves residual absorbance from the transformation products, and the EDC is reduced more efficiently due to the conversion of phenols into non-electron donating moieties (see discussion above). The overall fluorescence intensity decreased as fluorescent moieties are removed by reaction with O_3. The increase in Φ_f can be

441 explained by a model where absorbing moieties that are not fluoresceing are degraded
442 faster than fluorescing moieties, therefore the overall Φ_f values increase. For example,
443 electron-poor aromatic moieties (e.g., but not limited to, hydroxy aromatic ketones,
444 aldehydes, or acids) may not be abated efficiently by ozone under the chosen
445 experimental conditions due to their low second-order rate constants in comparison to
446 phenol (von Sonntag and von Gunten 2012). Fluorescence by these refractory
447 components would be less "diluted" from absorbance by non-fluorescing chromophores
448 that have reacted with ozone. Overall, this results in an increased Φ_f, for higher specific
449 ozone doses. These data indicate that a fraction of fluorophores within DOM are not
450 very reactive to ozone, and the overall fraction of fluorescent moieties in DOM is lower
451 than for absorbance.

452 *3.7 OH radical formation from ozone-DOM interaction*

453 Upon reaction of ozone with electron rich moieties of DOM (e.g., phenolic
454 moieties, amines, etc.), $^{\bullet}$OH can be formed by direct or indirect electron transfer
455 reactions to ozone (von Sonntag and von Gunten 2012). Table S4 summarizes published
456 $^{\bullet}$OH yields for a range of compounds: the $^{\bullet}$OH yield (amount of $^{\bullet}$OH formed relative to
457 consumed ozone) for e.g., both phenol and catechol was found to be 24% at pH 7
458 (Nöthe et al. 2009).

459 The cumulative $^{\bullet}$OH concentration was measured by formaldehyde formation
460 during ozonation of SRFA, NNOM and PLFA in presence of *t*-BuOH as a $^{\bullet}$OH
461 scavenger. Under these conditions, the stability of ozone is enhanced because chain
462 reactions are suppressed (Staehelin and Hoigné 1985). Therefore, these measurements
463 correspond to the primary $^{\bullet}$OH formation only and do not include chain reactions.

464 Figure 5 shows the cumulative $^{\bullet}$OH concentration as a function of time for

SRFA, NNOM, PLFA and phenol in the pH-range of 2-9 (data is shown for an ozone residual > 10% of initial ozone addition). In Figure S12, the cumulative $^{\bullet}$OH concentration is shown for longer reaction times. Generally, the cumulative $^{\bullet}$OH concentration increased during the first phase of the reaction, whereafter, it leveled off due to the depletion of the reactive moieties that lead directly to $^{\bullet}$OH formation. In absence of *t*-BuOH, re-formation of phenolic-type and other $^{\bullet}$OH-forming moieties could be expected by the reaction of $^{\bullet}$OH with aromatic sites (Nöthe et al. 2009). However, these reactions were suppressed under the applied experimental conditions.

Because the ozone depletion was slow both at pH 2 and 3, the consumption of the sites leading to $^{\bullet}$OH formation was slower and started to level off after 120s. Phenol was consumed in a relatively similair reaction time, faster at pH 3 than at pH 2. For pH 3, this leads to an earlier termination of the phenol-induced $^{\bullet}$OH formation (Figures 5a and b). At pH 7, the cumulative $^{\bullet}$OH concentration increased intially very sharply. The rate of depletion of the sites responsible for $^{\bullet}$OH formation decreased in the order phenol > SRFA > NNOM > PLFA (Figure 5c). At pH 9 the maximum cumulative $^{\bullet}$OH concentration was observed at 15s for both SRFA and NNOM, whereas for PLFA it gradually increased until 90s (Figure 5d).

The cumulative •OH formation can be compared with the ozone depletion kinetics in Figure 1: an initial drop in ozone depletion shown at 120s (pH 2 and 3) and at 90 and 15s (pH 7 and 9, respectively), corresponded to time points in Figure 5 where the cumulative •OH formation leveled off. These observations can be explained by the reactions between ozone and phenolic moieties consuming ozone instantly (Figure 1) and yielding •OH radicals (Figure 5).

(Figure 5)

Table 2 shows the •OH yields (maximum •OH concentration observed normalized to the ozone dose) as a function of the pH for SRFA, NNOM, PLFA and phenol, respectively and for a complete depletion of ozone. At pH 2, the •OH yields are 6.7%, 12.4% and 13.6% for SRFA, NNOM or PLFA, respectively. The yields observed at pH 3 (7.3%, 14.2%, 9.6% for SRFA, NNOM or PLFA, respectively) were all in reasonable agreement with the obtained yields for phenol at pH 2 and 3. At pH 7, the •OH yields were 27%, 30.5% or 21% for SRFA, NNOM or PLFA, respectively and at pH 9, they were about 33.7 and 38.6% for SRFA and NNOM, whereas for PLFA it was 28.5%. Hence, overall the •OH yields increase with increasing pH. This is in agreement with the higher •OH yields for phenol at pH 7 (37.5%) than at the lower pHs. Compared to a previous study the yields in this study were higher (compare 24% obained before with 28% obtained in this study, Table S4) (Flyunt et al. 2003).

At pH 7 and 9, the observed •OH yields for NNOM, SRFA and PLFA were quite similar. The trend for these yields are similar to the estimated phenol content of the respective DOM isolate (Table 1). However, it could be expected that NNOM, which only has about 70% of the phenol content of SRFA (compare 2.05 (NNOM) with 2.86 mmol phenol/g C (SRFA), respectively, Table 1), should have a smaller •OH yield for the same ozonation conditions. In the case of PLFA (1.77 mmol phenol/g C), the •OH yield corresponded to about 80% of the •OH yield of SRFA. The relatively high •OH yield for PLFA could be due to the higher content of amine-containing moieties, which may also be important sources for an indirect •OH formation via a superoxide radical-induced pathway (Buffle and von Gunten 2006).

(Table 2)

Figure S13 shows a correlation between the relative EDC abatement and the cumulative •OH yields for SRFA, NNOM and PLFA in the pH range 2-9. It is shown that the •OH yields are within certain limits proportional to the relative EDC abatement for all DOM types.

In summary, the results show that the •OH yields from ozone-DOM interactions significantly increase with increasing pH. Since the •OH yields do not vary significantly with varying pH amines may partly explain this trend (Mvula and von Sonntag 2003).

3.8 Effect of chlorination on EDC abatement

3.8.1 Changes in EDC as a function of the specific chlorine doses

We determined the changes in EDC and absorbance (254 and 280 nm) of SRFA, NNOM and PLFA as a function of an increasing chlorine dose at pH 7 (Figure S14). For all DOM isolates, the relative abatement of EDC is significantly more enhanced compared to the loss in the relative absorbance in comparison to the ozonation

527 experiments (compare Figure S14 with Figure 2 and Figures S8-S9). This is consistent
528 with previous findings (Wenk et al. 2013) and has been explained by the formation of
529 chlorinated phenolic moieties, which still have a significant UV absorbance while being
530 less redox active (Criquet et al. 2015, Deborde and von Gunten 2008, Wenk et al.
531 2013). To this end, Table S5 shows the molar absorption coefficients (ε) of the expected
532 chloriated reaction products (Gallard and von Gunten 2002, Lee and Morris 1962) at
533 254 or 280 nm, respectively, which were determined from the UV/Vis spectra in this
534 study (Figure S15). Despite the unknown product distribution during chlorination, a
535 strong absorbance can be expected, because most molar absorption coefficients (ε_{254} or
536 ε_{280nm}) are >2000 $M^{-1}cm^{-1}$ (Table S5). Compared to phenols, chlorophenols react more
537 slowly with chlorine to form non-absorbing products (Deborde and von Gunten 2008)
538 and because chlorophenols have significant UV absorbances, the slopes in plots of the
539 relative abatements of EDC versus UV absorbance are < -1.

540 *3.8.2 EDC abatement and correlaton with chloroform formation*

541 During chlorination, phenols and other activated aromatic moieties, such as
542 resorcinol (Norwood et al. 1980, Rebenne et al. 1996, Rook 1977, Theruvathu et al.
543 2001), but also β-diketo acid type moieties and β-diketones (Dickenson et al. 2008) can
544 serve as precursor for trihalomethanes (THMs, e.g., chloroform) formation. As
545 discussed above, the same activated aromatic compounds such as hydoxybenzenes react
546 readily with ozone (Hoigné and Bader 1983, von Sonntag and von Gunten 2012). As
547 hydroxybenzenes (including phenol/resorcinol moieties) also play an important role for
548 the EDC, the effect of EDC abatement on THM formation was assessed. To change the
549 EDC, pre-ozonation experiments were performed to abate EDC ≤ 95% in SRFA.
550 Chloroform and HAAs were then measured after post-chlorination of these samples.

551 Figure 6 shows the chloroform formation during post-chlorination as a function
552 of the relative EDC abatement. In most experiments (except 40 μM HOCl, Figure 6a), a
553 pronounced decrease in chloroform formation, was observed only for the pre-ozonated
554 samples with a realtive EDC of 50%. Similar observations were also apparent for the
555 formation of the haloacetic acids monochloroacetic acid (MCAA), dichloroacetic acid
556 (DCAA) or trichloroacetic acid (TCAA) (Figure S16). Once an abatement of EDC of
557 about 50% was reached, the $CHCl_3$ formation decreased. This threshold was reached
558 earlier for a higher chlorine dose (40 μM) because under these conditions chloroform
559 formation was precursor-limited and small changes in precursor concentrations led to a
560 decrease. In contrast, for smaller chlorine doses (≤ 25 μM) this effect was no longer
561 visible until a threshold EDC abatement was reached, because of the excess of
562 precursors relative to chlorine. In agreement to the current observations, no effect on
563 DBP formation (chloroform, TCAA and adsorbable organic chlorine) could be observed
564 from a DBP formation potential test during chlorination, after 10-40% EDC abatement
565 by ozone in a previous study (de Vera et al. 2017a). Therefore, the above-mentioned
566 results might be explained by a low extent of precursor abatement during pre-ozonation
567 for low relative EDC abatements.

568 The presence of *t*-BuOH during pre-ozonation blocks hydroxyl radical
569 oxidation, but also leads to higher ozone exposures compared to the absence of a
570 scavenger. The higher exposure may affect the chloroform formation during post-
571 chlorination, as demonstrated in a previous study in which an identical ozone dose was
572 applied with and without *t*-BuOH (De Vera et al. 2015). In contrast to these previous
573 results, the results obtained in presence and absence of *t*-BuOH are very similar in the
574 current study (Figures 6a and b). Based on these results, we conclude that $^{\bullet}OH$ only has
575 a limited effect on chloroform formation during post-chlorination. Similar conclusions

576 can be drawn from the formation of HAAs in presence and absence of *t*-BuOH (Figure
577 S16).

578 **(Figure 6)**

579 **4. Conclusions**

580 Based on results from ozone-DOM interactions in the pH-range 2-9 and
581 chlorine-DOM interactions at pH 7, it can be concluded that phenolic moiteies play a
582 dominant role for the DOM reactivity.

583 • The ozone depletion kinetics during ozonation of DOM was greatly affected by
584 changes in degree of protonation: The ozone depletion kinetics increased in the
585 pH-range 2-9, which could be explained by an important contribution of
586 phenolic moieties in the DOM.

587 • The pH-dependence of EDC-absorbance correlations during (i) ozonation
588 indicate a higher benzoquinone yield from the DOM oxidation at higher pH,
589 which is in agreement with results from ozone-phenol reactions. (ii) For
590 chlorine, a more efficient EDC abatement as compared to absorbance was
591 observed and could be explained by formation of strongly UV-absorbing
592 mono-, di- and/or trichlorophenols, which are not oxidized by the ABTS
593 radical cation.

594 • The fluorescence intensity decreased during ozonation, while an increase in
595 fluorescence quantum yield (Φ_f) was observed. The increase in Φ_f could not be
596 explained by benzoquinone formation, it is suggested to take place due to the
597 fast abatement of phenolic moieties relative to fluorophores with low ozone
598 reactivity.

599 • During ozonation, increasing $^{\bullet}$OH yields were observed with increasing pH (2-

600 9), as a result of the higher amine reactivity at higher pH.

601 • The relative abatement of EDC by pre-ozonation did not influence the
602 chloroform/chloroacetic acids formation during post-chlorination for relative
603 EDC abatements ≤ ~50% as long as the chloroform/chloroacetic acids
604 formation is not precursor limited. For EDC abatements > 50%, the
605 chloroform/chloroacetic acids (from post-chlorination) decrease was strongly
606 correlated with the ozone-induced EDC abatement.

5. Acknowledgements

LÖ acknowledges the Swedish Research Council, VR (grant number 2014-6839) for financial support. GM and FRO ackknowledge support from the US National Science Foundation (CBET #1453906). The authors also acknowledge Dr. Michael Sander for valuable comments on the manuscript.

6. References

Aeschbacher, M., Graf, C., Schwarzenbach, R.P. and Sander, M. (2012) Antioxidant Properties of Humic Substances. Environmental Science & Technology 46(9), 4916-4925.

Aeschbacher, M., Sander, M. and Schwarzenbach, R.P. (2010) Novel Electrochemical Approach to Assess the Redox Properties of Humic Substances. Environmental Science & Technology 44(1), 87-93.

Bader, H. and Hoigné, J. (1981) Determination of ozone in water by the indigo method. Water Research 15(4), 449-456.

Bourgin, M., Beck, B., Boehler, M., Borowska, E., Fleiner, J., Salhi, E., Teichler, R., von Gunten, U., Siegrist, H. and McArdell, C.S. (2018) Evaluation of a full-scale wastewater treatment plant upgraded with ozonation and biological post-treatments: Abatement of micropollutants, formation of transformation products and oxidation by-products. Water Research 129, 486-498.

Buffle, M.-O. and von Gunten, U. (2006) Phenols and Amine Induced HO• Generation During the Initial Phase of Natural Water Ozonation. Environmental Science & Technology 40(9), 3057-3063.

Cawley, K.M., Korak, J.A. and Rosario-Ortiz, F.L. (2014) Quantum Yields for the Formation of Reactive Intermediates from Dissolved Organic Matter Samples from the Suwannee River. Environmental Engineering Science 32(1), 31-37.

Chon, K., Salhi, E. and von Gunten, U. (2015) Combination of UV absorbance and electron donating capacity to assess degradation of micropollutants and formation of bromate during ozonation of wastewater effluents. Water Research 81, 388-397.

Criquet, J., Rodriguez, E.M., Allard, S., Wellauer, S., Salhi, E., Joll, C.A. and von Gunten, U. (2015) Reaction of bromine and chlorine with phenolic compounds and natural organic matter extracts – Electrophilic aromatic substitution and oxidation. Water Research 85, 476-486.

de Vera, G.A., Gernjak, W. and Radjenovic, J. (2017a) Predicting reactivity of model DOM compounds towards chlorine with mediated electrochemical oxidation. Water Research 114, 113-121.

de Vera, G.A., Gernjak, W., Weinberg, H., Farré, M.J., Keller, J. and von Gunten, U. (2017b) Kinetics and mechanisms of nitrate and ammonium formation during ozonation of dissolved organic nitrogen. Water Research 108, 451-461.

645 De Vera, G.A., Stalter, D., Gernjak, W., Weinberg, H.S., Keller, J. and Farré, M.J.
646 (2015) Towards reducing DBP formation potential of drinking water by favouring direct
647 ozone over hydroxyl radical reactions during ozonation. Water Research 87, 49-58.

648 Deborde, M. and von Gunten, U. (2008) Reactions of chlorine with inorganic and
649 organic compounds during water treatment - Kinetics and mechanisms: A critical
650 review. Water Research 42(1-2), 13-51.

651 Dickenson, E.R.V., Summers, R.S., Croué, J.-P. and Gallard, H. (2008) Haloacetic acid
652 and Trihalomethane Formation from the Chlorination and Bromination of Aliphatic β-
653 Dicarbonyl Acid Model Compounds. Environmental Science & Technology 42(9),
654 3226-3233.

655 Flyunt, R., Leitzke, A., Mark, G., Mvula, E., Reisz, E., Schick, R. and von Sonntag, C.
656 (2003) Determination of •OH, O2•-, and hydroperoxide yields in ozone reactions in
657 aqueous solution. The Journal of Physical Chemistry B 107(30), 7242-7253.

658 Gallard, H. and von Gunten, U. (2002) Chlorination of phenols: Kinetics and formation
659 of chloroform. Environmental Science & Technology 36(5), 884-890.

660 Garcia-Villanova, R.J., Garcia, C., Gomez, J.A., Garcia, M.P. and Ardanuy, R. (1997)
661 Formation, evolution and modeling of trihalomethanes in the drinking water of a town:
662 I. At the municipal treatment utilities. Water Research 31(6), 1299-1308.

663 Ge, F., Tang, F., Xu, Y. and Xiao, Y. (2014) Formation characteristics of haloacetic
664 acids from phenols in drinking water chlorination. Water Science and Technology-
665 Water Supply 14(1), 142-149.

666 Gerrity, D., Gamage, S., Jones, D., Korshin, G.V., Lee, Y., Pisarenko, A., Trenholm,
667 R.A., von Gunten, U., Wert, E.C. and Snyder, S.A. (2012) Development of surrogate
668 correlation models to predict trace organic contaminant oxidation and microbial
669 inactivation during ozonation. Water Research 46(19), 6257-6272.

670 Hammes, F., Salhi, E., Köster, O., Kaiser, H.-P., Egli, T. and von Gunten, U. (2006)
671 Mechanistic and kinetic evaluation of organic disinfection by-product and assimilable
672 organic carbon (AOC) formation during the ozonation of drinking water. Water
673 Research 40(12), 2275-2286.

674 Heeb, M.B., Kristiana, M., Trogolo, D., Arey, J.S. and von Gunten, U. (2017)
675 Formation and reactivity of inorganic and organic chloramines and bromamines during
676 oxidative water treatment. Water Research 110, 91-101.

677 Hoigné, J. and Bader, H. (1983) Rate constants of reactions of ozone with organic and
678 inorganic compounds in water—II. Water Research 17(2), 185-194.

679 Hoigné, J. and Bader, H. (1994) Characterization of water-quality criteria for ozonation
680 processes. 2. Lifetime of added ozone. Ozone-Science & Engineering 16(2), 121-134.

681 Huber, S.A., Balz, A., Abert, M. and Pronk, W. (2011) Characterisation of aquatic
682 humic and non-humic matter with size-exclusion chromatography - organic carbon
683 detection - organic nitrogen detection (LC-OCD-OND). Water Research 45(2), 879-
684 885.

685 IHSS (2017), International Humics Substance Society, http://humic-
686 substances.org/acidic-functional-groups-of-ihss-samples/.

687 Lakowicz, J.R. (2006) Principles of Fluorescence Spectroscopy, Springer, Baltimore,
688 USA.

689 Lee, G.F. and Morris, J.C. (1962) Kinetics of chlorination of chlorination of phenol-
690 chlorophenolic tastes and odors. International Journal of Air and Water Pollution 6(4),
691 419-431.

692 Lee, W., Westerhoff, P. and Croue, J.-P. (2007) Dissolved organic nitrogen as a
693 precursor for chloroform, dichloroacetonitrile, N-Nitrosodimethylamine, and
694 trichloronitromethane. Environmental Science & Technology 41(15), 5485-5490.

695 Lee, Y. and von Gunten, U. (2010) Oxidative transformation of micropollutants during
696 municipal wastewater treatment: Comparison of kinetic aspects of selective (chlorine,
697 chlorine dioxide, ferrate(VI), and ozone) and non-selective oxidants (hydroxyl radical).
698 Water Research 44(2), 555-566.

699 Lee, Y. and von Gunten, U. (2016) Advances in predicting organic contaminant
700 abatement during ozonation of municipal wastewater effluent: reaction kinetics,
701 transformation products, and changes of biological effects. Environmental Science-
702 Water Research & Technology 2(3), 421-442.

703 Leenheer, J.A. and Croue, J.P. (2003) Characterizing aquatic dissolved organic matter.
704 Environmental Science & Technology 37(1), 18A-26A.

705 Ma, J.H., Del Vecchio, R., Golanoski, K.S., Boyle, E.S. and Blough, N.V. (2010)
706 Optical Properties of Humic Substances and CDOM: Effects of Borohydride Reduction.
707 Environmental Science & Technology 44(14), 5395-5402.

708 McCurry, D.L., Quay, A.N. and Mitch, W.A. (2016) Ozone Promotes Chloropicrin
709 Formation by Oxidizing Amines to Nitro Compounds. Environmental Science &
710 Technology 50(3), 1209-1217.

711 McKay, G., Korak, J.A., Erickson, P.R., Latch, D.E., McNeill, K. and Rosario-Ortiz,
712 F.L. (2018) The Case Against Charge Transfer Interactions in Dissolved Organic Matter
713 Photophysics. Environmental Science & Technology 52(2), 406-414.

714 Mitch, W.A. and Sedlak, D.L. (2002) Formation of N-nitrosodimethylamine (NDMA)
715 from dimethylamine during chlorination. Environmental Science & Technology 36(4),
716 588-595.

717 Mvula, E. and von Sonntag, C. (2003) Ozonolysis of phenols in aqueous solution.
718 Organic & Biomolecular Chemistry 1(10), 1749-1756.

719 Nash, T. (1953) The Colorimetric Estimation of Formaldehyde by Means of the
720 Hantzsch Reaction. Biochemical Journal 55(3), 416-421.

721 Norwood, D.L., Johnson, J.D., Christman, R.F., Hass, J.R. and Bobenrieth, M.J. (1980)
722 Reactions of chlorine with selected aromatic models of aquatic humic material.
723 Environmental Science & Technology 14(2), 187-190.

724 Nöthe, T., Fahlenkamp, H. and Von Sonntag, C. (2009) Ozonation of wastewater: Rate
725 of ozone consumption and hydroxyl radical yield. Environmental Science and
726 Technology 43(15), 5990-5995.

727 Nowell, L.H. and Hoigné, J. (1992) Photolysis of aqueous chlorine at sunlight and
728 ultraviolet wavelengths. 1. Degradation rates. Water Research 26(5), 593-598.

729 Önnby, L., Walpen, N., Salhi, E., Sander, M. and von Gunten, U. (2018) Two analytical
730 approaches quantifying the electron donating capacities of dissolved organic matter to
731 monitor its oxidation during chlorination and ozonation. Resubmitted to Water
732 Research with minor revisions

733 Osburn, C.L., Handsel, L.T., Mikan, M.P., Paerl, H.W. and Montgomery, M.T. (2012)
734 Fluorescence Tracking of Dissolved and Particulate Organic Matter Quality in a River-
735 Dominated Estuary. Environmental Science & Technology 46(16), 8628-8636.

736 Pinkernell, U., Nowack, B., Gallard, H. and von Gunten, U. (2000) Methods for the
737 photometric determination of reactive bromine and chlorine species with ABTS. Water
738 Research 34(18), 4343-4350.

739 Ramseier, M.K. and von Gunten, U. (2009) Mechanisms of Phenol Ozonation-Kinetics
740 of Formation of Primary and Secondary Reaction Products. Ozone-Science &
741 Engineering 31(3), 201-215.

742 Rebenne, L.M., Gonzalez, A.C. and Olson, T.M. (1996) Aqueous Chlorination Kinetics
743 and Mechanism of Substituted Dihydroxybenzenes. Environmental Science &
744 Technology 30(7), 2235-2242.

745 Rook, J. (1977) Chlorination reactions of fulvic acids in natural waters. Environmental
746 Science & Technology 11(5), 478-482.

747 Shah, A.D., Liu, Z.-Q., Salhi, E., Hofer, T., Werschkun, B. and von Gunten, U. (2015)
748 Formation of disinfection by-products during ballast water treatment with ozone,
749 chlorine, and peracetic acid: influence of water quality parameters. Environmental
750 Science: Water Research & Technology 1(4), 465-480.

751 Sharpless, C.M. and Blough, N.V. (2014) The importance of charge-transfer
752 interactions in determining chromophoric dissolved organic matter (CDOM) optical and
753 photochemical properties. Environmental Science: Processes & Impacts 16(4), 654-671.

754 Song, Y., Breider, F., Ma, J. and von Gunten, U. (2017) Nitrate formation as a surrogate
755 parameter for abatement of micropollutants and the N-nitrosodimethylamine (NDMA)
756 formation potential during ozonation. submitted.

757 Staehelin, J. and Hoigné, J. (1985) Decomposition of ozone in water in the presence of
758 organic solutes acting as promoters and inhibitors of radical chain reactions.
759 Environmental Science & Technology 19(12), 1206-1213.

760 Stedmon, C.A., Markager, S. and Bro, R. (2003) Tracing dissolved organic matter in
761 aquatic environments using a new approach to fluorescence spectroscopy. Marine
762 Chemistry 82(3), 239-254.

763 Swietlik, J. and Sikorska, E. (2004) Application of fluorescence spectroscopy in the
764 studies of natural organic matter fractions reactivity with chlorine dioxide and ozone.
765 Water Research 38(17), 3791-3799.

766 Tentscher, P. and von Gunten, U. (2017) Ozonation of differently substituted model
767 phenolic compounds produces high yields of p-benzoquinones and other cyclic alpha,
768 beta-unsaturated ketones, in preparation.

769 Tentscher, P.R., Bourgin, M. and von Gunten, U. (2018) Ozonation of para-substituted
770 phenolic compounds yields p-benzoquinones, other alpha, beta, unsaturated ketones,
771 and substituted catechols. Environmental Science & Technology, in press.

772 Tentscher, P.R., Bourgin, M. and von Gunten, U. (2018) Ozonation of para-substituted
773 phenolic compounds yields p-benzoquinones, other alpha, beta unsaturated ketones, and
774 substituted catechols. Environmental Science & Technology, In press.

775 Theruvathu, J.A., Flyunt, R., Aravindakumar, C.T. and von Sonntag, C. (2001) Rate
776 constants of ozone reactions with DNA, its constituents and related compounds. Journal
777 of the Chemical Society-Perkin Transactions 2 (3), 269-274.

778 von Gunten, U. (2003) Ozonation of drinking water: Part II. Disinfection and by-
779 product formation in presence of bromide, iodide or chlorine. Water Research 37(7),
780 1469-1487.

781 von Sonntag, C. and von Gunten, U. (2012) Chemistry of ozone in water and
782 wastewater treatment: From basic principles to applications, IWA Publishing, London,
783 UK.

784 Walker, J.F. (1944) Formaldehyde, American Chemical Society, New York.

785 Walpen, N., Schroth, M.H. and Sander, M. (2016) Quantification of Phenolic
786 Antioxidant Moieties in Dissolved Organic Matter by Flow-Injection Analysis with
787 Electrochemical Detection. Environmental Science & Technology 50(12), 6423-6432.

788 Weishaar, J.L., Aiken, G.R., Bergamaschi, B.A., Fram, M.S., Fujii, R. and Mopper, K.
789 (2003) Evaluation of Specific Ultraviolet Absorbance as an Indicator of the Chemical
790 Composition and Reactivity of Dissolved Organic Carbon. Environmental Science &
791 Technology 37(20), 4702-4708.

792 Wenk, J., Aeschbacher, M., Salhi, E., Canonica, S., von Gunten, U. and Sander, M.
793 (2013) Chemical Oxidation of Dissolved Organic Matter by Chlorine Dioxide,
794 Chlorine, And Ozone: Effects on Its Optical and Antioxidant Properties. Environmental
795 Science & Technology 47(19), 11147-11156.

796 Wittmer, A., Heisele, A., McArdell, C.S., Bohler, M., Longree, P. and Siegrist, H.
797 (2015) Decreased UV absorbance as an indicator of micropollutant removal efficiency
798 in wastewater treated with ozone. Water Science and Technology 71(7), 980-985.

799 Zimmermann, S.G., Wittenwiler, M., Hollender, J., Krauss, M., Ort, C., Siegrist, H. and
800 von Gunten, U. (2011) Kinetic assessment and modeling of an ozonation step for full-
801 scale municipal wastewater treatment: Micropollutant oxidation, by-product formation
802 and disinfection. Water Research 45(2), 605-617.

803

Figure captions

Figure 1. Ozone depletion kinetics at an ozone:carbon molar ratio of 0.25:1 for SRFA, NNOM and PLFA at (a) pH 2, (b) pH 3, (c) pH 7, and (d) pH 9. Experimental conditions: 208 µM initial carbon concentration from the different model DOM isolates, 52 µM ozone, 100 mM *t*-BuOH and pH-adjusted H_2SO_4 (pH 2), 10 mM phosphate (pH 3, 7), 10 mM borate (pH 9). Samples were quenched with indigo at the specified reaction times to quantify the remaining concentration of ozone.

Figure 2. Relationship between the relative abatements of EDC and absorbance at 254 nm during the reaction of ozone with SRFA for a molar ozone:carbon ratio of 0.25:1 at (a) pH 2, (b) pH 3, (c) pH 7, and (d) pH 9. Samples were quenched with 0.1 mM sulfite (to measure changes in absorbance) or 1.0 mM maleic acid (to quantify EDC). Initial concentrations were 52 µM for ozone, 208 µM for carbon and 100 mM *t*-BuOH, respectively in pH-adjusted solutions with H_2SO_4 (pH 2), 10 mM phosphate (pH 3, 7), 10 mM borate (pH 9).

Figure 3. Absorbance spectra for phenol (34 µM) before (0 s) and after (60 s) reaction with ozone (52 µM) for an ozone:carbon molar ratio of 0.25:1 for (a) pH 2, (b) pH 3 and (c) pH 7 and with 100 mM *t*-BuOH. In (b) and (c) the spectra for 1,4-benzoquinone are also shown (with concentrations of (b) 10 µM, (c) 21 µM). The samples were quenched with 0.1 mM sulfite and adjusted for pH with H_2SO_4 (pH 2) or 10 mM phosphate (pH 3, 7). The absorbance at 254 nm is marked in the plots by a vertical line.

Figure 4. Relative changes in absorbance at 350 nm (values < 1) and the fluorescence quantum yield Φ_f/Φ_{f0} (values >1), as a function of (a) the specific ozone dose, and (b) the relative residual EDC. The experimental data represent the average of duplicates and error bars represent propagated standard deviations. Experimental conditions: 100 mM *t*-BuOH, 10 mM phosphate buffer (pH 7), initial carbon concentration 208 µM.

Figure 5. Evolution of the cumulative hydroxyl radical ($^{\bullet}OH$) concentrations (µM) for SRFA, NNOM, PLFA and phenol at an ozone:carbon molar ratio of 0.25:1. (a) pH 2, (b) pH 3, (c) pH 7 and (d) pH 9. Samples were quenched with 0.1 mM sulfite (1 mM sulfite for phenol). Experimental conditions: 208 µM initial carbon concentration, 100 mM *t*-BuOH, ozone dose = 52 µM, initial phenol concentration 34 µM, pH-adjusted with H_2SO_4 (pH 2), 10 mM phosphate (pH 3, 7) or 10 mM borate (pH 9).

Figure 6. Relative EDC abatements during pre-ozonation and the corresponding chloroform formation during post-chlorination of SRFA. Post-chlorination doses: 8, 16, 25 and 40 µM HOCl. (a) Presence of *t*-BuOH during pre-ozonation (closed circles), (b) absence of *t*-BuOH (open circles). Experimental conditions: DOC concentration = 208 µM, 10 mM phosphate buffer (pH=7), 100 mM *t*-BuOH. Data on EDC abatement are presented in Table S6.

Tables

Table 1. Phenol or aromaticity content (weight %) from EDC measurements[a] and IHSS[b], respectively. The ratio between phenol and the aromaticity, the absolute EDC (mmol e^-/g C) and the nitrogen and carbon content[b] (weight %) are also shown.

	SRFA	**NNOM**	**PLFA**
Phenol, %[a]	26.9±6.72	19.3±3.57	16.7±2.29
Phenol, mmol phenol/g C[b]	2.86±0.71	2.05±0.38	1.77±0.24
Aromaticity, %[c]	22.0	19.0	12.0
(Phenol/aromaticity)	1.22	1.01	1.39
EDC, mmol e-/g C[d]	5.98	4.16	2.43
C, %[e]	52.3	53.2	52.5
N, %[e]	1.17	1.10	6.51

[a]Phenol content from EDC measurements was calculated by using the approach from (Aeschbacher et al. 2012), details on calculations are found in Text S5), [b]Phenol content from the phenol estimates from the EDC measurements in this study, [c]determined by ^{13}C-NMR estimates of carbon distribution and obtained from IHSS: www.humicsubstances.org, [d]EDC values recalculated from (Aeschbacher et al. 2012), [e]carbon and nitrogen content from elemental composition in % (w/w) of a dry, ash-free sample, elemental composition obtained from IHSS: www.humicsubstances.org.

Table 2. $^{\bullet}$OH yields from the reactions of SRFA, NNOM, PLFA or phenol with ozone in the pH range 2-9 at an ozone:carbon molar ratio of 0.25:1.0. Initial carbon concentration 208 μM, ozone dose 52 μM, and in presence of 100 mM *t*-BuOH. The presented values are averaged for triplicate measurements and the standard deviations are rounded off to one significant digit.

	$^{\bullet}$OH **yield, (%)[a]**			
	pH 2	**pH 3**	**pH 7**	**pH 9**
SRFA	6.7±0.8	7.3±0.4	27.0±1.2	33.7±1.5
NNOM	12.4±1.4	14.2±1.5	30.5±0.9	38.6±0.7
PLFA	13.6±0.4	9.6±1.1	21.0±0.1	28.5±0.3
Phenol	6.6±0.0	6.6±0.0	37.5±0.1	na[b]

[a]OH radical yield normalized to the ozone dose, [b]na: not applicable.

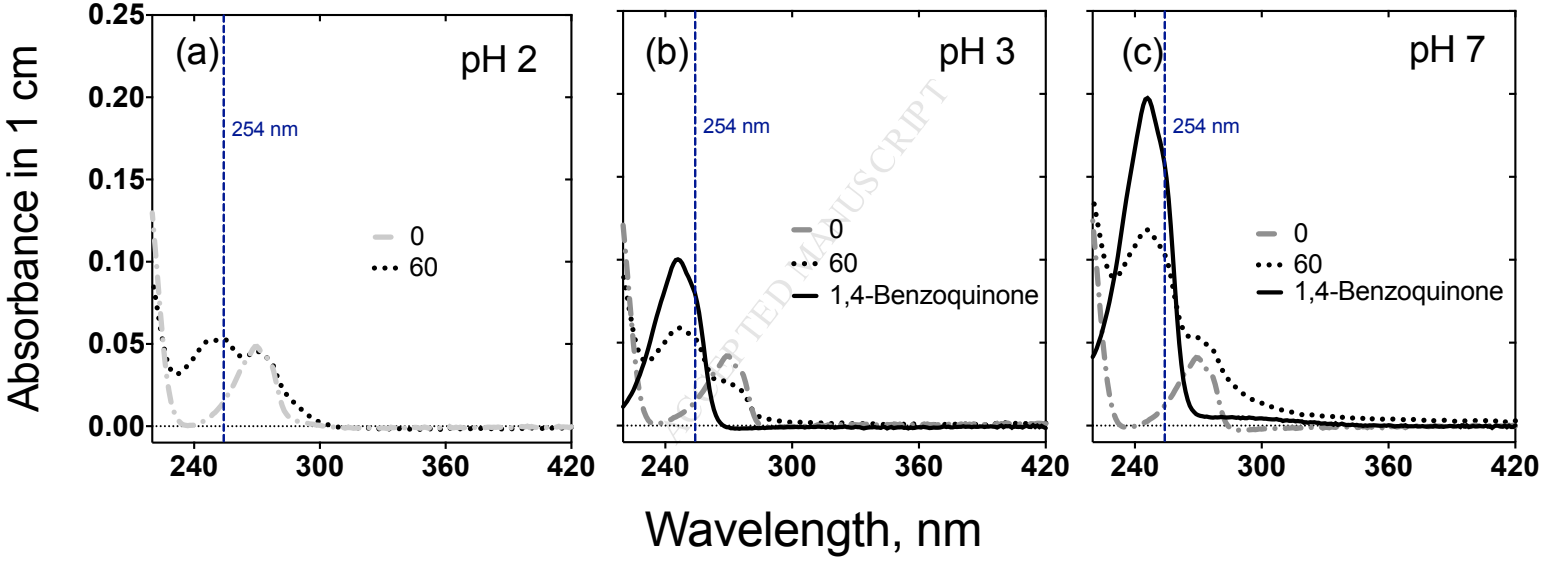

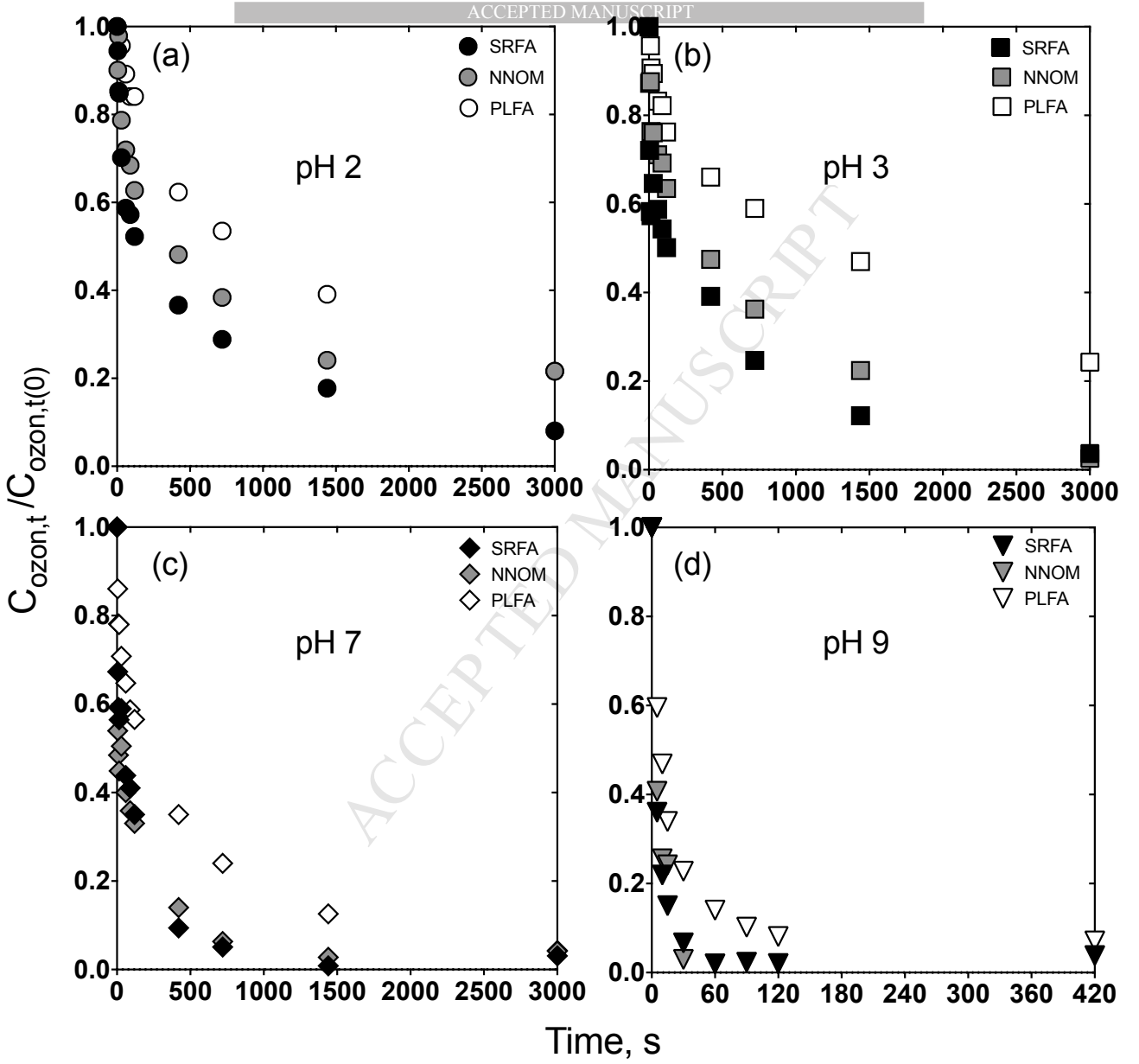

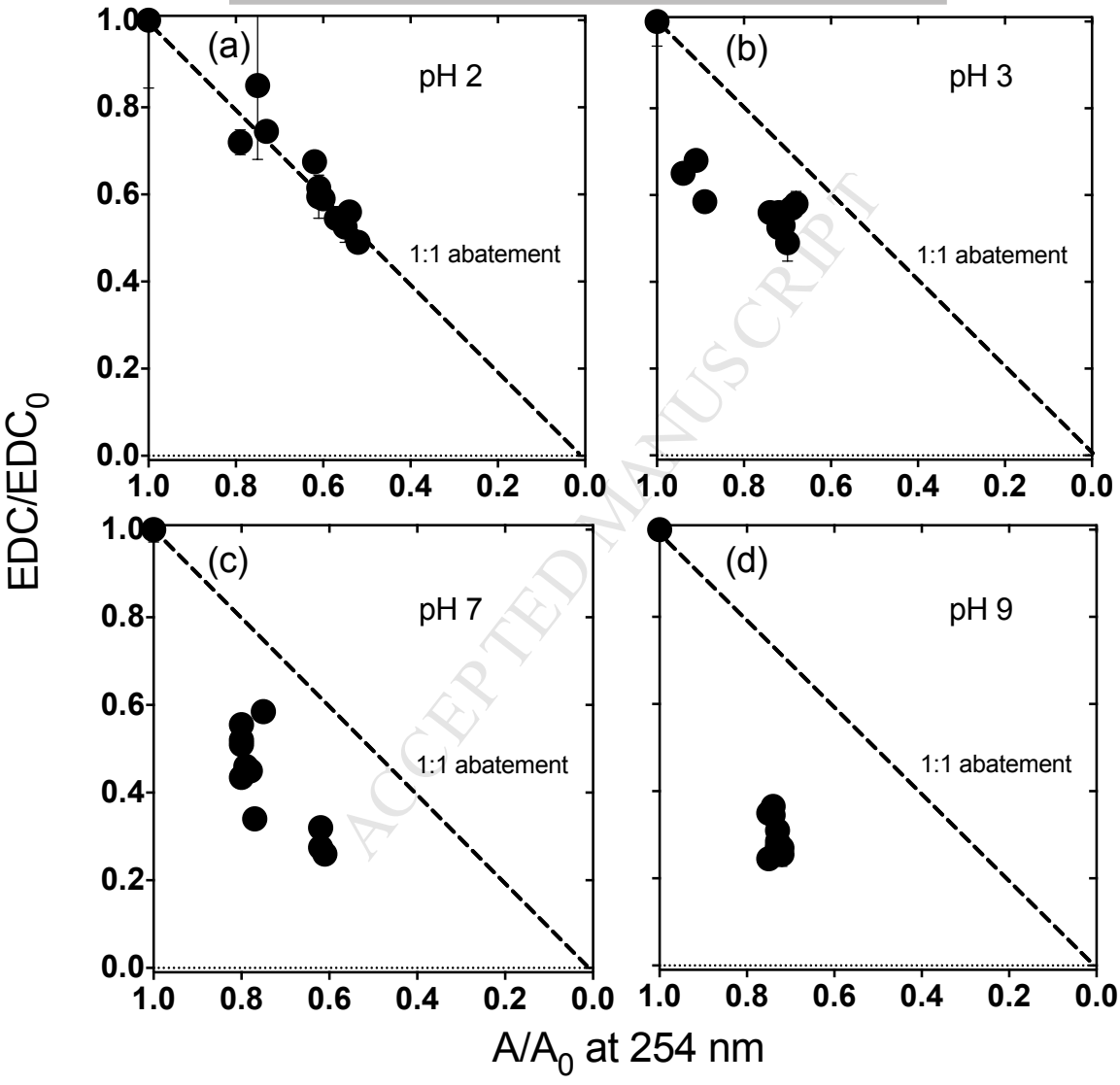

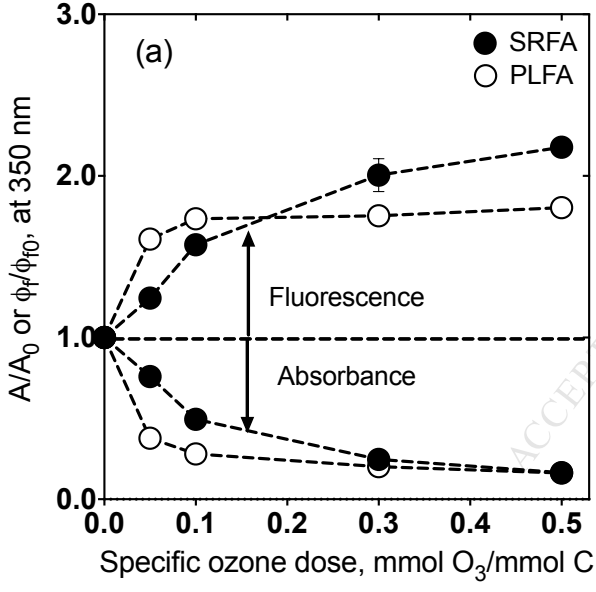

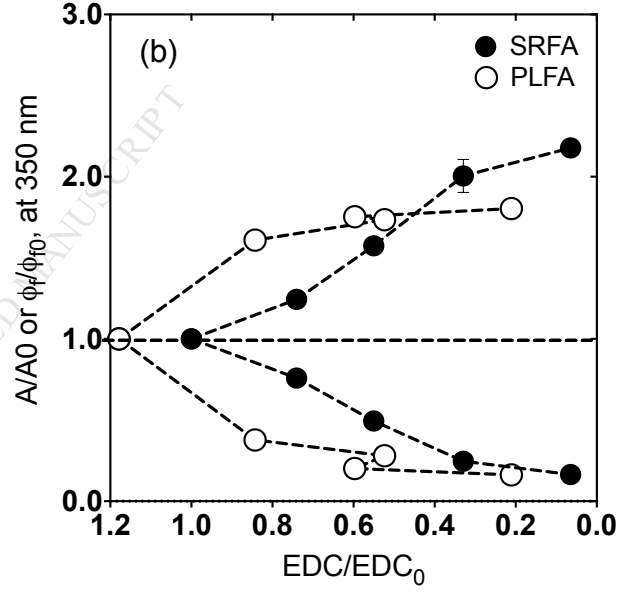

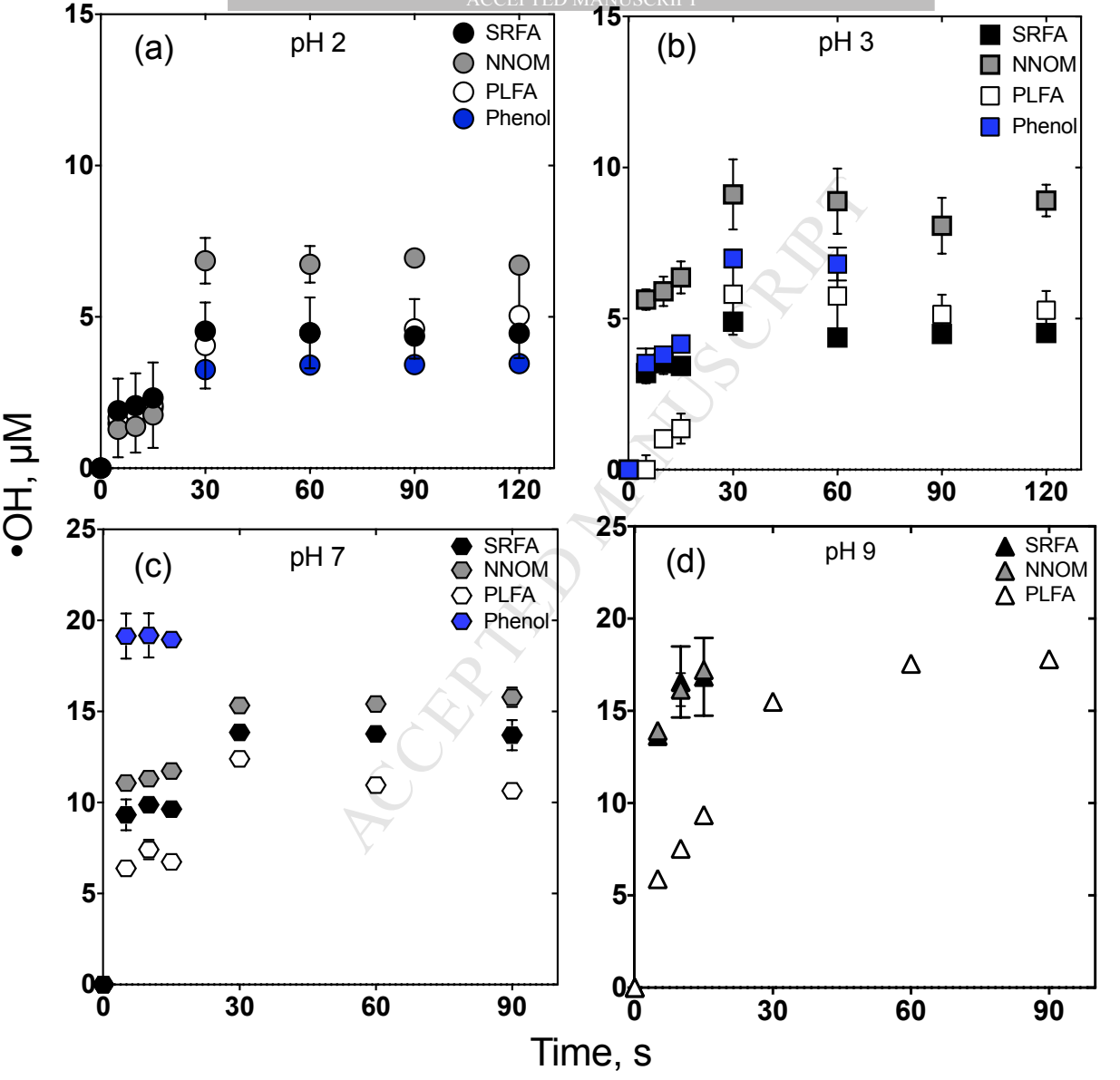

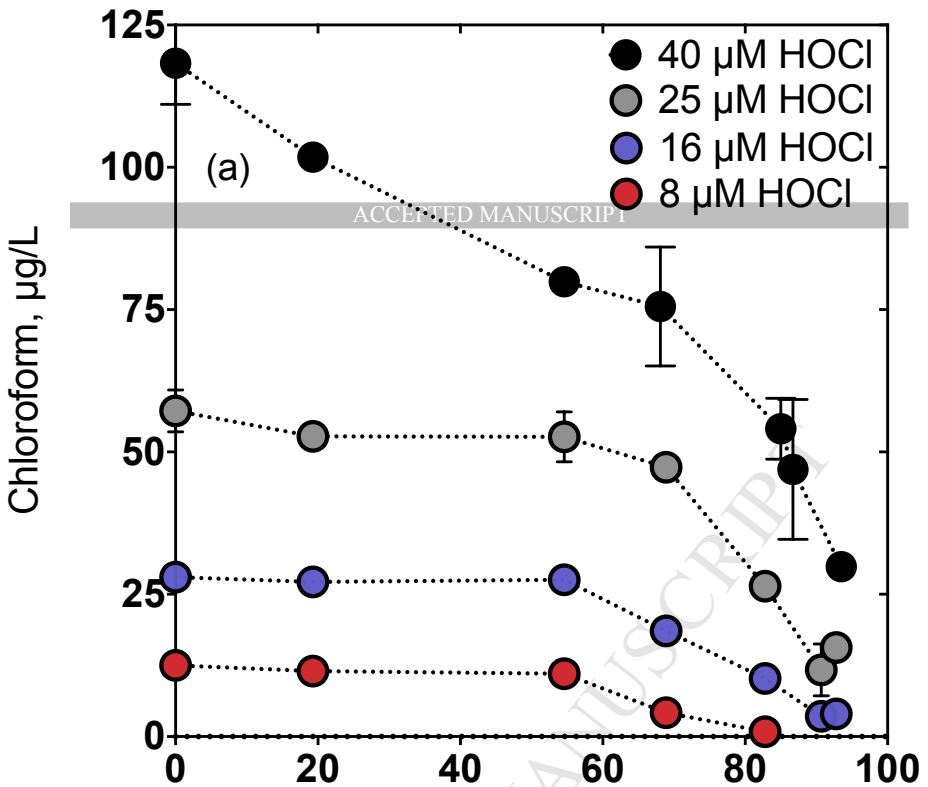

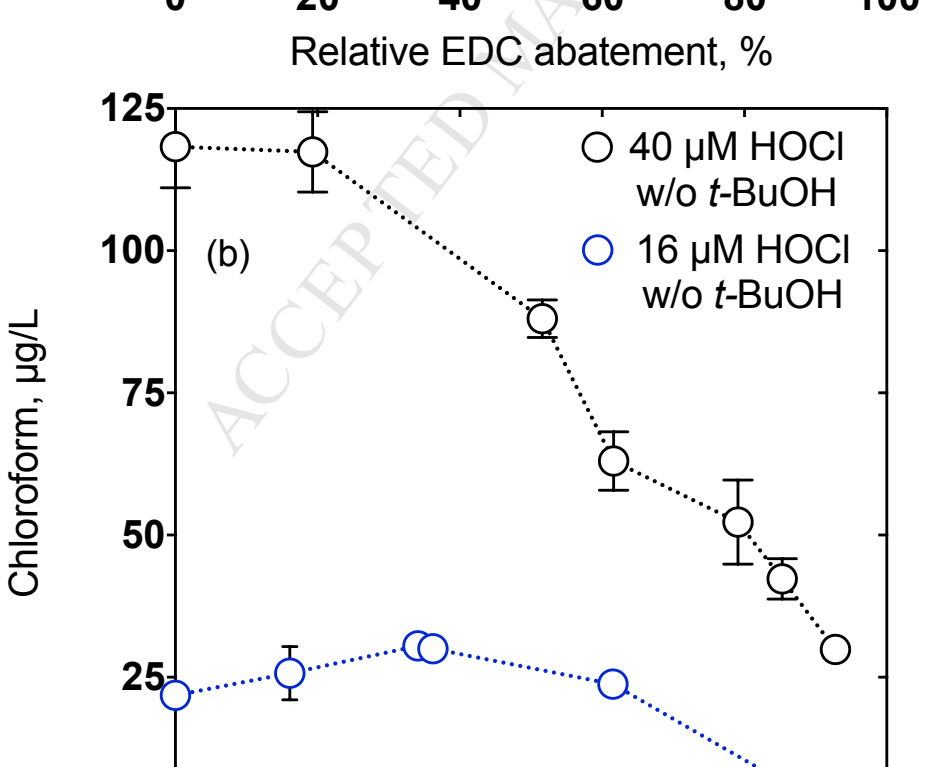

Highlights

- Ozone (O_3)- and chlorine-DOM reactions were assessed in the pH range 2-9
- For O_3, the relationship between EDC and absorbance is pH dependent
- For O_3, benzoquinone formation explained low absorbance/high EDC loss at pH>7
- For chlorine, UV-absorbing chlorophenols were formed while EDC decreased
- $CHCl_3$ formation during chlorination of DOM decreased for > ~50% EDC abatement